[PS]Documenting Mudstone Heterogeneity by Use of Principal Component Analysis of X-Ray Diffraction and Portable X-Ray Fluorescence Data: A Case Study in the Triassic Shublik Formation, Alaska North Slope*

A. Boehlke[1], K. J. Whidden[2], and W. Benzel[2]

Search and Discovery Article #51355 (2017)**
Posted February 6, 2017

*Adapted from poster presentation given at SEPM-AAPG 2016 Hedberg Research Conference, Santa Fe, New Mexico, October 16-19, 2016

[1]Central Energy Resources Science Center, U.S. Geological Survey, Denver, CO (aboehlke@usgs.gov)
[2]Central Energy Resources Science Center, U.S. Geological Survey, Denver, CO

Abstract

Determining the chemical and mineralogical variability within fine-grained mudrocks poses analytical challenges but is potentially useful for documenting subtle stratigraphic differences in physicochemical environments that may influence petroleum reservoir properties and behavior. In this study, we investigate the utility of combining principal component analysis (PCA) of X-ray diffraction (XRD) data and portable X-ray fluorescence (pXRF) data to identify simplifying relationships within a large number of samples and subsequently evaluate a subset that encompasses the full spectrum or range of mineral and chemical variability within a vertical section. Samples were collected and analyzed from a vertical core of the Shublik Formation, a heterogeneous, phosphate-rich, calcareous mudstone-to-marl unit deposited in the Arctic Alaska Basin (AAB) during the Middle and Late Triassic. The Shublik is a major petroleum source rock in the Alaskan North Slope, and is considered a prime target for continuous self-sourced resource plays.

Eighty samples were collected from a 10-m core interval of the Ikpikpuk-1 well (drilled in the National Petroleum Reserve in Alaska (NPRA)). Samples were ground to 250 micrometer size, and XRD data collected over the range 5° to 65° two-theta (2θ). These "rough" diffraction scans were analyzed as x-y data (2θ vs. intensity) using a cluster analysis algorithm included with PANalytical HighScore Plus software which evaluated both the peak profile (intensity) and peak positions (2θ spacing). The PCA identified seven simplifying relationship clusters among the samples that best describe the mineralogical variability within the entire XRD sample set without any pattern processing or interpretation from the analyst (Figure 1a). After removal of outliers from the seven-cluster PCA, a second PCA was run, setting the actual cutoff determination to the same value as was determined for the seven-cluster result (96.17%). The resulting PCA identified three clusters (Figure 1b) and further detailed analysis was conducted using this three cluster result.

The total variation encompassed within each cluster can be represented by three samples; the minimum-mean-distance sample (the most representative data point in a cluster), and two samples at the edges of each cluster which represent maximum and minimum values of variability. Three such samples from each cluster were evaluated by semi-quantitative XRD RockJock whole-pattern-fitting analysis (Eberl,

2003). Cluster 1 represents clay-rich samples with little dolomite; Cluster 2 consists of samples with more abundant dolomite and apatite contents; and Cluster 3 is composed of samples dominated by calcite (Table 1).

Semi-quantitative XRD was performed on each of the remaining samples to confirm that the mineralogical differences indicated by PCA analysis and summarized by the nine representative samples were consistent and reasonable within expected tolerances. For example, mean dolomite abundances for Clusters 1, 2, and 3 are 3.6, 8.8, and 0.4 wt. %, respectively, based on semi-quantitative XRD, which compares with the respective minimum-mean-distance dolomite values from the XRD-PCA of 1.1, 11, and 0 wt. %. A similar relationship is seen for all minerals, including clay and phosphate minerals (Table 1). Inspection of the XRD-PCA results indicates Cluster 1 and Cluster 2 account for 78% of the variance in the sample set and 96% of variance is represented when Cluster 3 is included. This shows that the combination of "rough XRD" analysis (e.g., non-micronized samples, no internal standard, and no attempt at qualitative or quantitative interpretation) coupled with PCA to determine representative sample sets and further describe mineralogical variability. In this particular case study, 9 samples were able to represent a similar statistical distribution obtained from analysis of 80 samples.

Portable-XRF analysis was performed on all samples and multivariate PCA was applied to explain the variance in Ca, Al, Si, Fe, Mn, K, and Ti elemental concentrations. Both the XRD-PCA and pXRF-PCA distributions share some similarities; however, the outliers determined by the different PCA methods differ, as noted from one exception (Ikpikpuk 10298.6), which is the most siliceous sample, containing nearly 60% quartz, 10% feldspar, and 10% clay. This observation is reasonable as one would not expect the same samples to represent mean, maximum, and minimum variances when considering different types of data (compositional versus mineralogical). Principal Component-1(PC-1) and PC-2 account for over 96% of the elemental variance in the sample set. The pXRF-PCA data grouped all samples into a single, large calcium-dominated group, and variability within that group is represented by different loadings of Al, Si, Fe, Mn, and Ti on PC-1 and PC-2. Although pXRF data complements the XRD-PCA data by characterizing elemental relationships within certain rock types, it fails to adequately capture major element variation within a carbonate system which would aid in correlating rock types. This analysis method fails in our study due to high variation of Mg and P concentrations in our samples (and other mudstones) and the poor accuracy and precision in measuring these elements by pXRF.

The most clay-rich sample from each of the three XRD-PCA clusters was selected for oriented clay mineral analysis. Two of the three clay-rich samples with notably different clay mineralogy and total organic carbon contents were examined using scanning electron microscopy (SEM). Notable differences in the clay mineralogy exist between the three PCA clusters. Cluster 2 and Cluster 3 contain expandable illite/smectite (I/S); whereas Cluster 1 contained mostly or only illite. All of the samples are from approximately 10 m of core, so differences in burial depth and thermal maturity cannot account for the differences in clay mineralogy.

In carbonate-rich and phosphate-rich zones, the chemistry of the I/S is K^+ and Ca^{2+} bearing with some Mg^{2+}. In samples where Fe-chlorite is present the mixed-layer, I/S clays are still K^+ bearing, but have less Ca^{2+} and Mg^{2+} and more Fe^{2+}. This enrichment of Fe^{2+} in coexisting clay minerals is consistent with the burial diagenesis model of Newman (1987):

[mixed-layer I/S (ml_1) + K^+ (feldspar) -> illite (in mixed-layers)]
and

[kaolinite + illite + mixed-layer I/S (ml_1) + Fe^{2+} -> chlorite + mixed-layer I/S (ml_2)]

where, (ml_1) is the Ca^{2+} bearing mixed-layer I/S while (ml_2) is the Fe^{2+} bearing mixed-layer I/S. Chlorite and Fe^{2+} bearing I/S are only seen in samples containing relatively abundant pyrite, which suggests a chemically reducing pore water environment. XRD analysis of the less-than 2μm size fraction of a sample investigated by SEM-Energy Dispersive Spectroscopy confirmed the presence of both Fe-chlorite and mixed-layer I/S.

Mineralogical variability indicated by PCA analysis of XRD data appears to be independent of microscopically observed variations in rock texture or faunal remains that are more directly tied to variations in depositional conditions. Plotting the cluster assignment of each sample as a function of sample depth reveals a pattern of mineralogical variation that may relate to changes in pore water chemistry. For example, samples assigned to Cluster 1 (clay-rich) only occur below a depth of 10,287 feet; whereas samples assigned to Cluster 2 (dolomite and apatite-rich) only occur above this depth. Samples assigned to Cluster 3 (calcite-rich) occur throughout the 10-m core interval. The results of this study indicate that PCA analysis of XRD data can be used to summarize patterns of mineralogical variability that would otherwise go unrecognized in very fine-grained rocks. Documentation of this mineralogical variability is useful in discerning changes in depositional environment and sediment diagenesis during sedimentary basin evolution.

Disclaimer: Any use of trade, product, or firm names is for descriptive purposes only and does not imply endorsement by the U.S. Government.

References Cited

Eberl, D.D, 2003, User's Guide to RockJock: A Program for Determining Quantitative Mineralogy from Powder X-ray Diffraction Data. U.S. Geological Survey, Reston, VA, Open-File Report 03-78, 47 p.

Newman, A.C.D., 1987, Chemistry of Clays and Clay Minerals: Wiley, New York, NY, 480 p.

Documenting mudstone heterogeneity by use of principal component analysis of x-ray diffraction and portable x-ray fluorescence data: A case study in the Triassic Shublik Formation, Alaska North Slope.

Boehlke, A., Whidden, K.J., and Benzel, W., Central Energy Resources Science Center, U.S. Geological Survey, Denver, CO 80225

Determining the chemical and mineralogical variability within fine-grained mudrocks poses analytical challenges but is potentially useful for documenting subtle stratigraphic differences in physicochemical environments that may influence petroleum reservoir properties and behavior. In this study, we investigate the utility of combining principal component analysis (PCA) of X-ray diffraction (XRD) data and portable X-ray fluorescence (pXRF) data to identify simplifying relationships within a large number of samples and subsequently evaluate a subset that encompasses the full spectrum or range of mineral and chemical variability within a vertical section. Samples were collected and analyzed from a vertical core of the Shublik Formation, a heterogeneous, phosphate-rich, calcareous mudstone-to-marl unit deposited in the Arctic Alaska Basin (AAB) during the Middle and Late Triassic. The Shublik is a major petroleum source rock in the Alaskan North Slope, and is considered a prime target for continuous self-sourced resource plays.

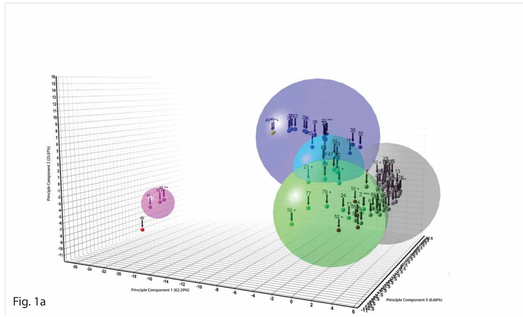

Fig. 1a

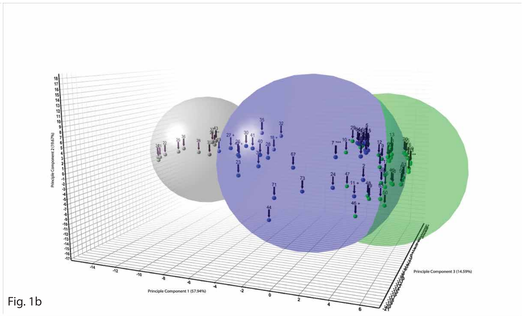

Fig. 1b

Mineral distributions statistically determined by measuring each sample (n=83)

Cluster	Qualifier	TOC	NON-CLAYS	Quartz	Plagioclase - albite	Calcite	Dolomite	Ankerite	Total Carbonate	Pyrite	Gypsum	Bassanite	Apatite	Total non-clays	CLAYS	Illite (1Md)	Fe-Chlorite	Total clays	TOTAL
1	Minimum	0.58		10.30	2.00	10.90	0.00	0.00	14.40	0.00				0.00	76.20	0.00		0.00	99.80
1	Median	2.40		16.90	4.20	56.80	3.80	0.00	61.30	2.40				7.50	90.10	9.50		9.90	100.00
1	Max	4.26		58.10	9.50	74.00	6.70	2.60	75.90	4.60				19.30	100.00	23.60		23.60	100.10
1	Average	2.30		19.34	4.75	52.59	3.59	0.46	56.64	2.57				6.16	89.45	10.52		10.54	99.99
1	Avg. Dev	0.76		5.90	1.76	12.90	1.29	0.66	12.72	0.77				4.16	5.01	5.01		5.00	0.06
	Count = 25																		
2	Minimum	1.36		8.00	1.40	16.90	0.80	0.00	26.80	1.00	0.28	1.16	8.80	85.30		0.00		0.00	99.90
2	Median	2.35		16.10	4.10	41.80	8.10	0.60	54.40	2.50	0.28	1.16	18.60	96.00		4.00		4.00	100.00
2	Max	3.55		24.30	15.40	62.70	18.50	4.50	73.10	6.00	0.28	1.16	52.70	100.74		14.70		14.70	100.74
2	Average	2.48		15.11	4.87	42.19	8.81	0.82	51.82	2.72	0.28	1.16	20.52	95.09		4.93		4.93	100.02
2	Avg. Dev	0.44		3.30	1.97	10.46	4.68	0.79	8.44	0.81	0.00	0.00	6.08	2.97		2.95		2.95	0.08
	Count = 34																		
3	Minimum	0.32		2.40	0.00	60.70	0.00	0.00	61.30	0.00				0.00	96.80	0.00		0.00	99.90
3	Median	1.40		4.45	0.40	89.00	0.00	0.55	91.40	0.60				1.85	99.20	0.80		0.80	100.00
3	Max	2.08		32.70	1.30	97.60	2.60	3.30	97.60	1.50				12.80	100.00	3.10		3.10	100.10
3	Average	1.26		7.02	0.47	86.64	0.42	1.17	88.23	0.54				2.68	98.94	1.05		1.05	99.99
3	Avg. Dev	0.54		4.50	0.39	6.33	0.58	1.16	6.36	0.41				2.58	0.91	0.89		0.89	0.02
	Count = 16																		

PCA Determined mineral distributions (n=9)

E-Sample ID	Field ID	Cluster	Qualifier	TOC	NON-CLAYS	Quartz	Plagioclase - albite	Calcite	Dolomite	Ankerite	Total Carbonate	Pyrite	Gypsum	Bassanite	Apatite	Total non-clays	CLAYS	Illite (1Md)	Fe-Chlorite	Total clays	Inorganic wt.%
E120404-030	10283.70	1	Minimum mean sam	3.16		18.60	5.40	50.40	1.10	2.20	53.70	1.70				5.90	85.30	14.70		14.70	100.00
E120404-034	10285.40	1	edge sample	2.50		16.90	6.90	26.60	4.10	0.00	30.70	3.30				19.30	77.10	22.90	Trace	22.90	100.00
E120404-050	10289.80	1	edge sample	2.39		12.60	3.40	74.00	1.80	0.00	75.80	2.60				0.00	94.40	5.60		5.60	100.00
			Count = 25																		
E120404-118	10276.20	2	Minimum mean sam	2.67		17.00	4.90	43.60	11.00	0.00	54.60	2.60				18.90	98.00	2.00		2.00	100.00
E120404-033	10284.50	2	edge sample	2.86		8.00	1.40	59.90	0.80	2.20	62.90	1.00				24.30	97.60	2.30		2.30	99.90
E120404-102	10271.70	2	edge sample	2.44		18.10	8.00	17.10	18.30	1.90	37.30	4.20				18.60	86.20	13.80		13.80	100.00
			Count = 34																		
E120404-043	10288.00	3	Minimum mean sam	1.06		4.00	0.10	91.40	0.00	0.10	91.50	0.00				4.40	100.00	0.00		0.00	100.00
E120404-041	10287.00	3	edge sample	1.93		4.70	0.70	79.60	0.00	2.20	81.80	0.00				12.80	100.00	0.00		0.00	100.00
E120404-070	10297.50	3	edge sample	0.32		32.70	1.30	60.70	0.00	0.60	61.30	1.20				1.90	98.40	1.60		1.60	100.00
			Count = 16																		

Table 1

Methods :

Eighty samples were collected from a 10-m core interval of the Ikpikpuk-1 well (drilled in the National Petroleum Reserve in Alaska (NPRA)). Samples were ground to 250 micrometer size, and XRD data collected over the range 5° to 65° two-theta (2θ). Scans were analyzed as x-y data (2θ vs. intensity) using a cluster analysis algorithm included with PANalytical HighScore Plus software which evaluated both the peak profile (intensity) and peak positions (2θ spacing). The PCA identified seven simplifying relationship clusters among the samples (Figure 1a). After removal of outliers from the seven-cluster PCA, a second PCA was run, setting the actual cutoff determination to the same value as was determined for the seven-cluster result (96.17%). The resulting PCA identified three clusters (Figure 1b) which describe the total variation encompassed within each cluster and can be represented by three samples; the minimum-mean-distance sample (the most representative data point in a cluster), and two samples at the edges of each cluster which represent maximum and minimum values of variability. Three such samples from each cluster were evaluated by semi-quantitative XRD RockJock whole-pattern-fitting analysis (Eberl, 2003). Cluster 1 represents clay-rich samples with little dolomite; Cluster 2 consists of samples with more abundant dolomite and apatite contents; and Cluster 3 is composed of samples dominated by calcite (Table 1). Portable-XRF analysis was performed on all samples and multivariate PCA was applied to explain the variance in Ca, Al, Si, Fe, Mn, K and Ti elemental concentrations (Figure 2) . The outliers determined by the different PCA methods differ, as noted from one exception (Ikpikpuk 10298.6), which is the most siliceous sample, containing nearly 60% quartz, 10% feldspar and 10% clay. This observation is reasonable as one would not expect the same samples to represent mean, maximum, and minimum variances when considering different types of data (compositional versus mineralogical). Principal Component-1(PC-1) and PC-2 account for over 96% of the elemental variance in the sample set. The pXRF-PCA data grouped all samples into a single, large calcium-dominated group, and variability within that group is represented by different loadings of Al, Si, Fe, Mn, and Ti on PC-1 and PC-2. Although pXRF data complements the XRD-PCA data by characterizing elemental relationships within certain rock types, it fails to adequately capture major element variation within a carbonate system which would aid in correlating rock types. This analysis method fails in our study due to high variation of Mg and P concentrations in our samples (and other mudstones) and the poor accuracy and precision in measuring these elements by pXRF.

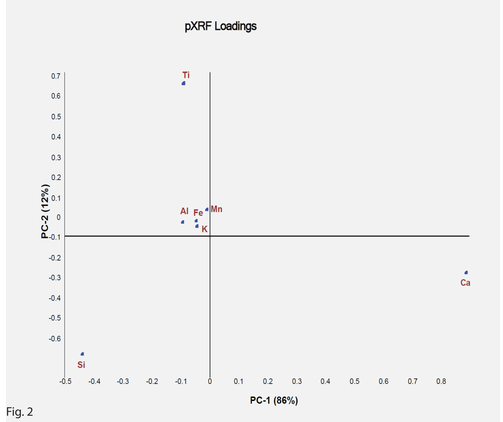

Fig. 2

The most clay-rich sample from each of the three XRD-PCA clusters was selected for oriented clay mineral analysis. Two of the three clay-rich samples with notably different clay mineralogy and total organic carbon contents were examined using scanning electron microscopy (SEM). Notable differences in the clay mineralogy exist between the three PCA clusters. Cluster 2 and Cluster 3 contain expandable illite/smectite (I/S); whereas Cluster 1 contained mostly or only illite. All of the samples are from approximately 10 m of core, so differences in burial depth and thermal maturity cannot account for the differences in clay mineralogy.

In carbonate-rich and phosphate-rich zones, the chemistry of the I/S is K^+ and Ca^{2+} bearing with some Mg^{2+}. In samples where Fe-chlorite is present the mixed-layer, I/S clays are still K^+ bearing, but have less Ca^{2+} and Mg^{2+} and more Fe^{2+}. This enrichment of Fe^{2+} in coexisting clay minerals is consistent with the burial diagenesis model of Newman (1987):

[mixed-layer I/S (ml_1) + K^+ (feldspar) -> illite (in mixed-layers)]
and
[kaolinite + illite + mixed-layer I/S (ml_1) + Fe^{2+} -> chlorite + mixed-layer I/S (ml_2)]

where, (ml_1) is the Ca^{2+} bearing mixed-layer I/S while (ml_2) is the Fe^{2+} bearing mixed-layer I/S. Chlorite (Figure 3)and Fe^{2+} bearing I/S are only seen in samples containing relatively abundant pyrite, which suggests a chemically reducing pore water environment.

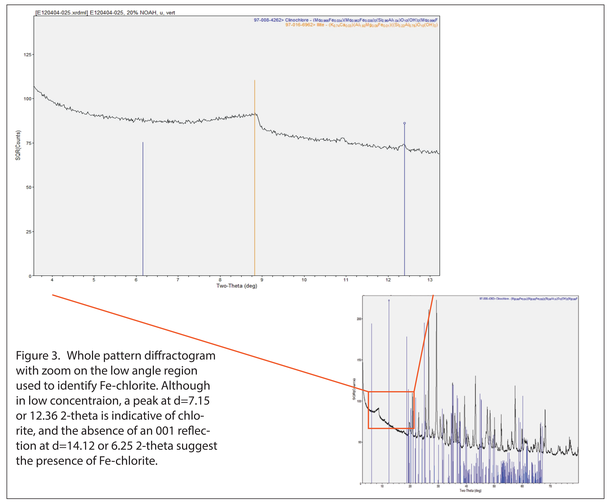

Figure 3. Whole pattern diffractogram with zoom on the low angle region used to identify Fe-chlorite. Although in low concentraion, a peak at d=7.15 or 12.36 2-theta is indicative of chlorite, and the absence of an 001 reflection at d=14.12 or 6.25 2-theta suggest the presence of Fe-chlorite.

Figure 5. Plotting the cluster assignment of each sample as a function of sample depth reveals a pattern of mineralogical variation that may relate to changes in pore water chemistry and/or paleo-redox conditions. For example, samples assigned to Cluster 1 (clay-rich) occur throughout the core, yet are concentrated at a depth above 10,287 feet. Samples assigned to Cluster 2 (dolomite and apatite-rich) occur above the 10287' depth and are concentrated in the upper section of the core between 10271.5' and 10277' with one exception at 10290'. Samples assigned to Cluster 3 (calcite-rich) only occur below the 10287' depth and are concentrated between 10287' and 10292.6'. Samples belonging to cluster 3 correlate well with the most reduced section of the core when the molar ratio of V/Cr measured by ICP-MS/AES is used as a proxy for paleo-redox conditions.

Summary

Results of this study indicate that PCA analysis of XRD data can be used to summarize patterns of mineralogical variability that would otherwise go unrecognized in very fine-grained rocks. Documentation of this mineralogical variability is useful in discerning changes in depositional environment and sediment diagenesis during sedimentary basin evolution.

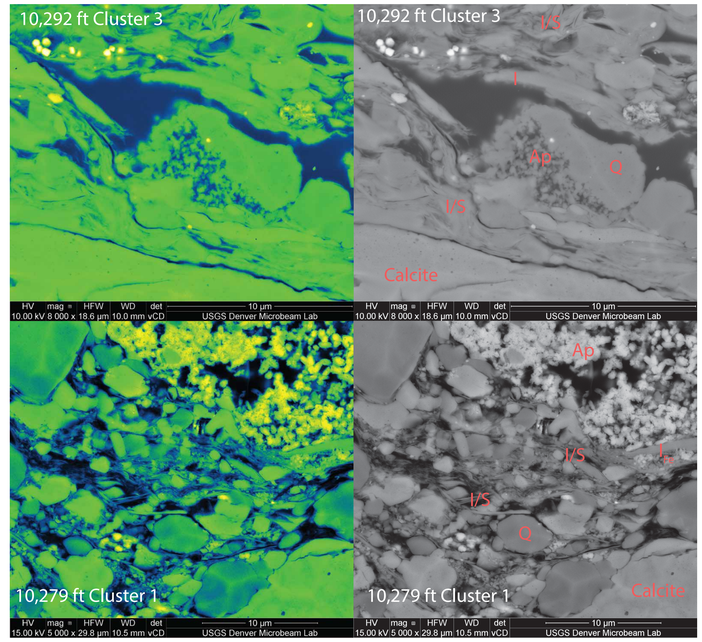

Figure 4. SEM Images of samples selected from clusters 1 and 3. Images on the left are ImageJ pseudo-color conversions of the backscatter image on the right. This pseudo-color conversion enhances the grayscale image by assigning color from a look up table to the shades of gray produced in an 8 bit image. The color conversion is meant to accentuate the difference in mineralogy from the two cluster groups, specifically the clay mineralogy. Not only do mineral percentages and chemistry analyzed by eds differ, the habit of which those minerals are distributed also differ.

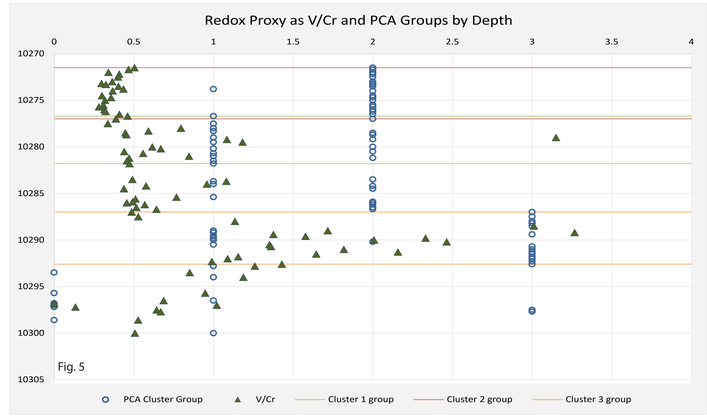

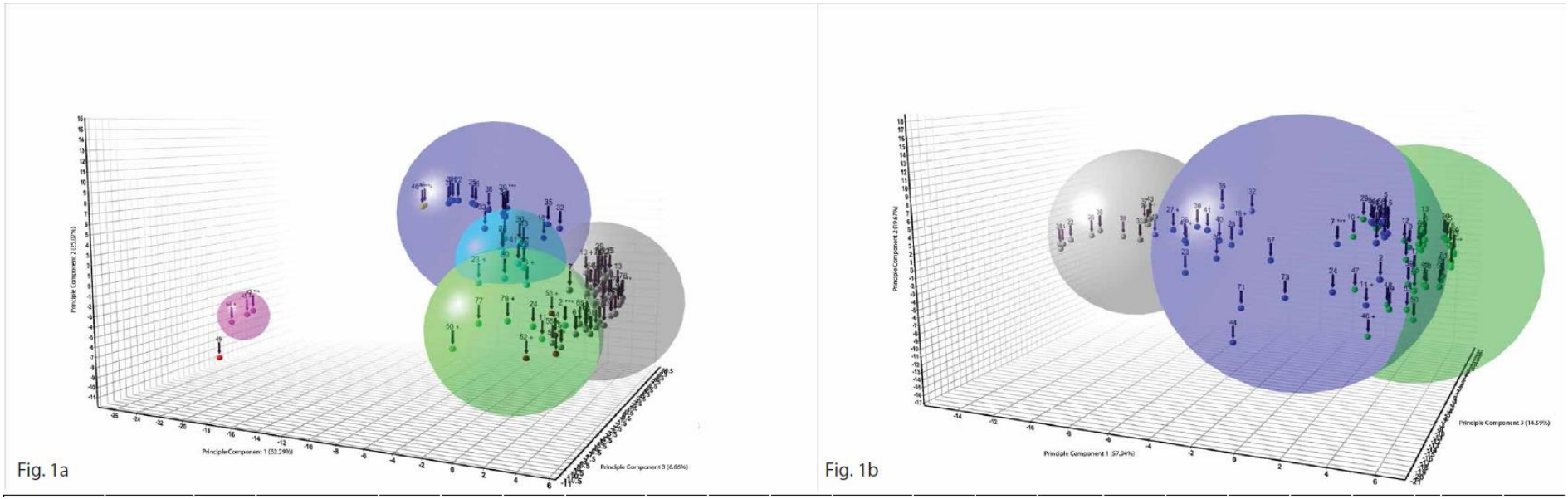

Figure 1. A) A seven-cluster dendogram cutoff with outliers on the negative side of PC-1 and clusters of the remaining samples on the positive end of PC-1. B.) This cluster grouping is a result of removing the outliers from the seven-cluster PCA and using the same dendogram cutoff value that was used in that PCA.

Table 1.

PCA Determined mineral distributions (n=9)

E-Sample ID	Field ID	Cluster		TOC	NON-CLAYS	Quartz	Plagioclase albite	Calcite	Dolomite	Ankerite	Total Carbonate	Pyrite	Gypsum	Bassanite	Apatite	Total non-CLAYS	Illite	Total clays	TOTAL Inorganic wt.%
E120404-030	10283,7	1	Minimum mean sample	3,157		18,6	5,4	50,4	1,1	2,2	53,7	1,7			5,9	85,3	14,7	14,7	100
E120404-034	10285,4	1	edge sample	2,498		16,9	6,9	26,6	4,1	0	30,7	3,3			19,3	77,1	22,9	22,9	100
E120404-050	10289,8	1	edge sample	2,394		12,6	3,4	74	1,8	0	75,8	2,6			0	94,4	5,6	5,6	100
E120404-118	10276,2	2	Minimum mean sample	2,67		17	4,9	43,6	11	0	54,6	2,6			18,9	98	2	2	100
E120404-033	10284,5	2	edge sample	2,863		8	1,4	59,9	0,8	2,2	62,9	1			24,3	97,6	2,3	2,3	99,9
E120404-102	10271,7	2	edge sample	2,44		18,1	8	17,1	18,3	1,9	37,3	4,2			18,6	86,2	13,8	13,8	100
E120404-043	10288,0	3	Minimum mean sample	1,058		4	0,1	91,4	0	0,1	91,5	0			4,4	100	0	0	100
E120404-041	10287,0	3	edge sample	1,928		4,7	0,7	79,6	0	2,2	81,8	0			12,8	100	0	0	100
E120404-070	10297,5	3	edge sample	0,324		32,7	1,3	60,7	0	0,6	61,3	1,2			1,9	98,4	1,6	1,6	100

Mineral distributions statistically determined by measuring each sample (n=80)

Cluster		TOC	NON-CLAYS	Quartz	Plagioclase albite	Calcite	Dolomite	Ankerite	Total Carbonate	Pyrite	Gypsum	Bassanite	Apatite	Total non-CLAYS	Illite	Total clays	TOTAL
1	Minimum	0,6		10,3	2,0	10,9	0,0	0,0	14,4	0,0			0,0	76,2	0,0	0,0	100
1	Median	2,4		16,9	4,2	56,8	3,8	0,0	61,3	2,4			7,5	90,1	9,5	9,9	100
1	Max	4,3		58,1	9,5	74,0	6,7	2,6	75,9	4,6			19,3	100,0	23,6	23,6	100
1	Average	2,3		19,3	4,7	52,6	3,6	0,5	56,6	2,6			6,2	89,5	10,5	10,5	100
1	Avg. Dev	0,8		5,9	1,8	12,9	1,3	0,7	12,7	0,8			4,2	5,0	5,0	5,0	0
2	Minimum	1,4		8,0	1,4	16,9	0,8	0,0	26,8	1,0	0,3	1,2	8,8	85,3	0,0	0,0	100
2	Median	2,3		16,1	4,1	41,8	8,1	0,6	54,4	2,5	0,3	1,2	18,6	96,0	4,0	4,0	100
2	Max	3,6		24,3	15,4	62,7	18,5	4,5	73,1	6,0	0,3	1,2	52,7	100,7	14,7	14,7	101
2	Average	2,5		15,1	4,9	42,2	8,8	0,8	51,8	2,7	0,3	1,2	20,5	95,1	4,9	4,9	100
2	Avg. Dev	0,4		3,3	2,0	10,5	4,7	0,8	8,4	0,8	0,0	0,0	6,1	3,0	2,9	2,9	0
3	Minimum	0,3		2,4	0,0	60,7	0,0	0,0	61,3	0,0			0,0	96,8	0,0	0,0	100
3	Median	1,4		4,5	0,4	89,0	0,0	0,6	91,4	0,6			1,9	99,2	0,8	0,8	100
3	Max	2,1		32,7	1,3	97,6	2,6	3,3	97,6	1,5			12,8	100,0	3,1	3,1	100
3	Average	1,3		7,0	0,5	86,6	0,4	1,2	88,2	0,5			2,7	98,9	1,1	1,1	100
3	Avg. Dev	0,5		4,5	0,4	6,3	0,6	1,2	6,4	0,4			2,6	0,9	0,9	0,9	0

Table 1. Mineral Distribution.